

EFFECT OF VARYING THE DOUBLE RADIAL SWIRLER CONFIGURATION ON THE FLUID DYNAMIC AND EMISSIONS PERFORMANCES IN A CAN COMBUSTOR

Mohd Najib Md Zainul^a, Mohammad Nazri Mohd Jaafar^{a,b*}, Tholudin Mat Lazim^a

^aDepartment of Aeronautical, Automotive & Ocean Engineering, Faculty of Mechanical Engineering, Universiti Teknologi Malaysia, 81310 UTM Johor Bahru, Johor, Malaysia

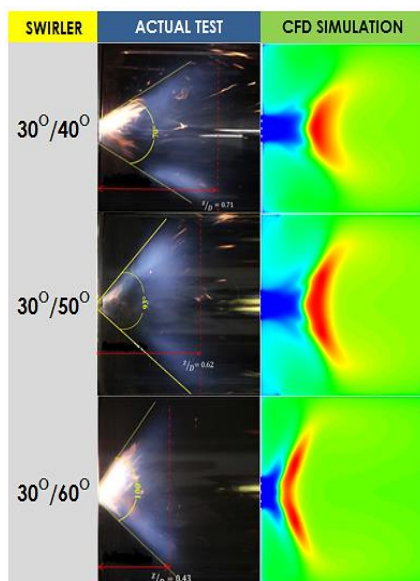
^bInstitute for Vehicle System and Engineering, Universiti Teknologi Malaysia, 81310 UTM Johor Bahru, Johor, Malaysia

Article history

Received
21 January 2017
Received in revised form
31 May 2017
Accepted
17 August 2017

*Corresponding author
nazri@mail.fkm.utm.my

Graphical abstract



Abstract

The main purpose of this article is to present the fluid dynamic and combustion performances of a can combustor applying double radial flow swirler. Analysis was conducted using Computational Fluid Dynamics simulation (CFD) and compared with experimental works conducted by previous researchers. Air pollution, in the form of gaseous emissions from gas turbine generator reportedly increasing every year. Design modifications was identified and used in this study where air swirler been proven able to reduce the formation rate of gaseous emission such as NO_x and CO during combustion. Swirler in a burner is a device that serves to improve the air and fuel mixture in the main combustion zone. Swirlers, presently studied are from a combination of two radial swirlers with different vane angle (primary and secondary) such as 30°/40°, 30°/50° and 30°/60°. Application of Ansys Fluent 14 CFD solvers was used in this study. Turbulent flow model used was from Reynolds Average Navier-Stokes (RANS) type involving k-ε. The fuel used is diesel. The parameters studied were wall temperature distribution along the combustor, the volume of NO_x and volume of CO in the main combustion zone. Results from this study showed that the combination of 30°/60° generates the lowest gaseous emissions production rate. The highest average percentage error obtained by simulation studies compared to the actual experimental values for NO_x was 22% and CO was 17.8%. Comparison between simulation and actual study proves that the simulation method can be used for preliminary decision and able to be used as benchmark to determine which is the best swirler configuration.

Keywords: Double radial swirler, swirl number, NO_x, CO, CFD simulation

© 2017 Penerbit UTM Press. All rights reserved

1.0 INTRODUCTION

The air pollution caused by air transportation and power station has shown gradual increment every year. The consequence of this issue was that the emission control regulation have been stricter. The high cost equipment required for conducting experimental work limits the study for emission in the combustor experimentally. In addition, there are lack of data in previous studies by other researchers that present the behavior of fluid

dynamics in a combustion chamber before and during the combustion.

The main purpose of this study is to compare the data of experimental works done for double swirler performance with combustion simulation. Next is to find the best simulation model that produce the most similar result compared to experiment.

The simulation work will use Computational Fluid Dynamic (CFD) method whereas the turbulence model

selected was the Reynolds Averaging Navier-Stokes (RANS).

Swirling flow is a phenomenon in a combustor that creates an adequate air and fuel mixture during combustion. Fuel injection and mixing efficiency are very important factors for combustion besides gas turbine efficiency [1]. The swirl strength measured is in term of Swirl number.

The swirl number should, if possible, be determined from measured values of velocity and static pressure profiles [2]. Notably, the swirl number controls swirling flames and that any changes in the values of swirl number have important impact on the flame dynamics [3]. This flame stabilization can be achieved by creation of a toroidal reversal flow that entrains and recirculates a portion of the combustible gases to mix with the incoming fresh air and fuel mixture [4].

This study presents a flow field effect in a can combustor that uses double radial swirlers. Swirler is a flame holder that swirls the flow of incoming air and fuel [5]. This swirler combination consists of primary and secondary vanes that practically generate an additional turbulence flow in the combustor primary zone. The double radial swirler combination that used in this study consists of 30°/40°, 30°/50° and 30°/60° vane angles combinations [6]. Figure 1 and Table 1 show the design and specification dimensions for the radial swirler used in this study.

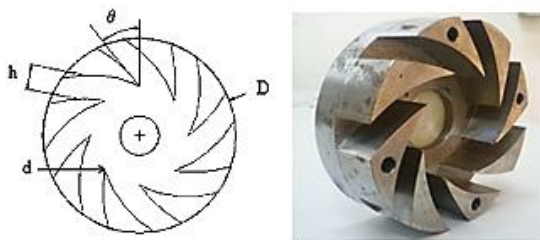


Figure 1 Radial swirler design

Two radial swirlers were combined together and placed at the inlet of the combustor. Each swirler separated at certain distance by using a sleeve in order to distinguish the turbulence effect between swirlers at the air inlet. The air inlet source for both swirlers is the same but has a gap in between them as shown in Figure 2.

Table 1 Specification of the radial swirlers

Swirler Angle θ	30	40	50	60
Parameter				
Channel width, h (mm)	13.6	12.3	11.2	9.6
Outer Diameter, D (mm)	98			
Inner Diameter, d (mm)	50			
Vane Depth L (mm)	25			
Swirl number, S_n	0.366	0.630	0.978	1.427

Appropriate combustion control is necessary to prevent flashback and oscillating combustion [7]. In order to get a desired performance in the combustor during combustion, it is important that we can maintain or increase the swirl strength. This improvement needs to be developed and controlled in the fluid dynamics and combustion studies. A good air/fuel mixing process is achievable by producing a strong swirling flow. To study a swirling flow, we need to understand the velocity profile and its pattern. In the combustor there exist two types of swirl that are asymmetrical fuel inlet and swirl-stabilized. However, when the asymmetric fuel inlet was used, the resulting flame had absolutely different characteristics than the swirl-stabilized flames [8].

Velocity profile and turbulence intensity are the criteria that show a significant value for measuring the performance and mixture of air/fuel in combustor. Studies in turbulence or vortex flow in combustor sometime will pose difficulty to analysts. The turbulent premixed flames found in industrial gas turbine combustors are difficult to study due to high levels of turbulence, fast chemistry and complex geometrical features [9].

Without swirler, the velocity will only be riveted to axial components and not spreading the mixing fluid to complete the area of combustion. The combustion flame size and pattern is depending on the momentum of air/fuel. The momentum flux ratio can play an important role in altering the flow and flame structures [10]. If the flow velocity increased to become jet, we can observe a strong flame appearance. To anchor and increase flame stability, the central recirculation zone is desirable.

Flame stabilization in a swirl combustor is achieved by forming a relatively low-pressure region in the downstream of the swirler as the result of the swirling flow entrainment [11]. In this zone, where vortex breakdown is generated, backflow to the burner is induced and the flow phenomenon is called flow recirculation [12].

The importance of this condition is that it will pull back the flow close to the inlet and enhance the mixing of the substances. This process will increase the completeness of combustion and reduce the emission production such as Carbon Monoxide and Unburned Hydrocarbon. The combination of short distance, formation of a flame, short residence time during combustion and high flame temperature could reduce the formation of CO and NOx [13]. The fluid characteristic in cold and combustion scenario is different in term of density and viscosity. The increment of temperature will reduce the density of the working fluid.

A combustion simulation in CFD is a challenging process. The reaction between turbulent structures and chemical reactions features a multi-scale non-linear problem [14]. In CFD, the most common and efficient parallel computing strategy is to decompose the original problem into a set of tasks [15].

The research gap for this study is that there is no numerical comparison for double swirler flow characteristic, such as flame and velocity profile

comparisons. Experimental investigation of gas turbine combustion is difficult and can provide only limited information due to practical limitations [16].

Hence, the objective of this study is to find the best turbulence model that predicts closest to actual experimental results and to find the best combination of double swirler that give the utmost reduction of emissions.

2.0 METHODOLOGY

2.1 Actual testing

Figure 2 shows the arrangement of test rig for combustion in the actual testing. The performance of this design has been tested in the actual combustion-testing rig.

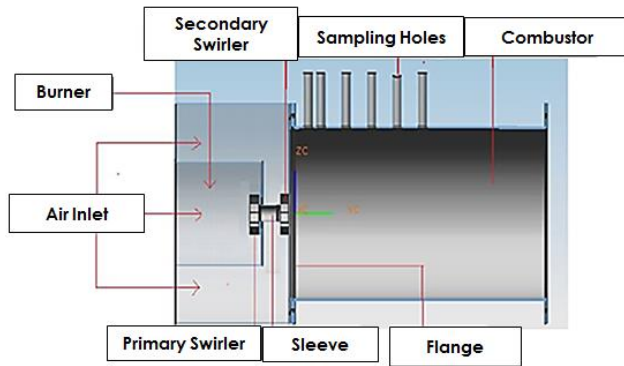


Figure 2 The arrangement of double radial swirler in can combustor testing rig [6]

2.2 Mathematical Model

Swirl number (Sn) is a dimensionless value that represents how strong the swirl is in certain flow. Al Kabie [17] has described the swirl number (Sn) as;

$$Sn = \frac{\sin\theta}{1 + \frac{1}{\tan\theta}} \left[\frac{A_a}{C_c A_{th}} \right] \quad (1)$$

where

A_a is the exit area

A_{th} is the swirler minimum throat area

C_c is the swirler contraction coefficient

In the dynamic fundamental, Beer [18] also formulated a swirl number as;

$$Sn = \frac{G_\theta}{RG_z} \quad (2)$$

where

G_θ is the tangential flux momentum

G_z is the axial flux momentum

R is the swirler radius

For this analysis, the flow is to be considered incompressible and turbulent. The fundamental of CFD analysis is the governing equations and transport equations. The governing equations are mathematically consisting of the conservation of mass, momentum and energy. These models derived in the following equations (3, 4 and 5) as;

$$\frac{\partial \rho}{\partial t} + \frac{\partial}{\partial x_i} (\rho \vec{u}_i) = 0 \quad (3)$$

$$\frac{\partial}{\partial t} (\rho \vec{u}_i) + \frac{\partial}{\partial x_i} (\rho \vec{u}_i \vec{u}_j) = -\frac{\partial p}{\partial x_i} + \frac{\partial}{\partial x_j} \left[\mu \left(\frac{\partial \vec{u}_i}{\partial x_j} + \frac{\partial \vec{u}_j}{\partial x_i} - \frac{2}{3} \delta_{ij} \frac{\partial \vec{u}_k}{\partial x_k} \right) + \frac{\partial}{\partial j} \left(-\frac{\tau_{ij}}{\rho u_i u_j} \right) \right] \quad (4)$$

$$\rho \frac{\partial}{\partial x_i} (V(E + p)) = \frac{\partial}{\partial x_i} (k_{eff} \nabla T - h\psi + \bar{t}V) \quad (5)$$

The species transport equations described in equation (6) as below,

$$\frac{\partial}{\partial t} \int_v \rho \phi dV + \oint_A \rho \phi V \cdot dA = \oint_A \Gamma_\phi \nabla \phi \cdot dA - \int_v S_\phi dV \quad (6)$$

2.3 CFD Model

This simulation was conducted using actual dimension of a can combustor model. The CFD domain consists of the space that was filled by airflow and combustion products. At the swirler area, the vane channel for the air inlet was inverted to a CFD domain. In the actual physical of combustion model, all fluid space converted to a solid with a boundary condition properties applied that will be used for CFD simulation as shown in Figure 3. The flow field characteristic measured at several cross sections (z/D).

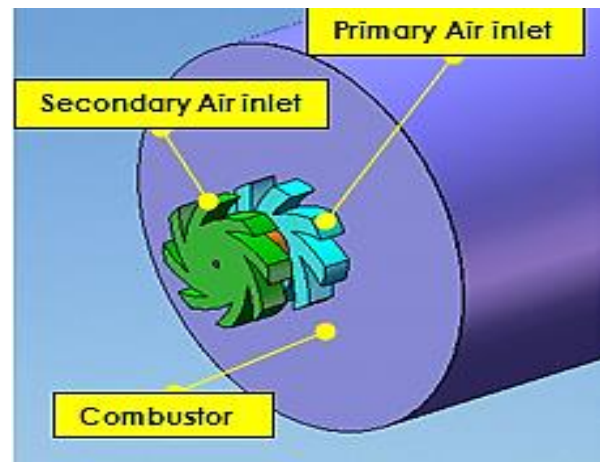


Figure 3 CFD geometry for double swirler

2.2.1 Meshing

In order to run simulation work, two figures of meshing/grid size were drawn and generated (Figures 4 and 5). It is necessary to make sure to select which is the optimum number of meshing cell required and able to produce the most accurate and dependable CFD representation for study justification. Table 2 shows three different grid sizes that were generated using ANSYS14.0 ICEM CFD.

Table 2 Grid sizes used in Grid independency test

Grid	Number of cell	Minimum cell area [m ²]	Maximum cell area [m ²]
G1	643,146	8.67×10^{-6}	7.92×10^{-3}
G2	924,582	1.25×10^{-7}	1.23×10^{-4}
G3	1,323,666	2.96×10^{-9}	3.49×10^{-5}

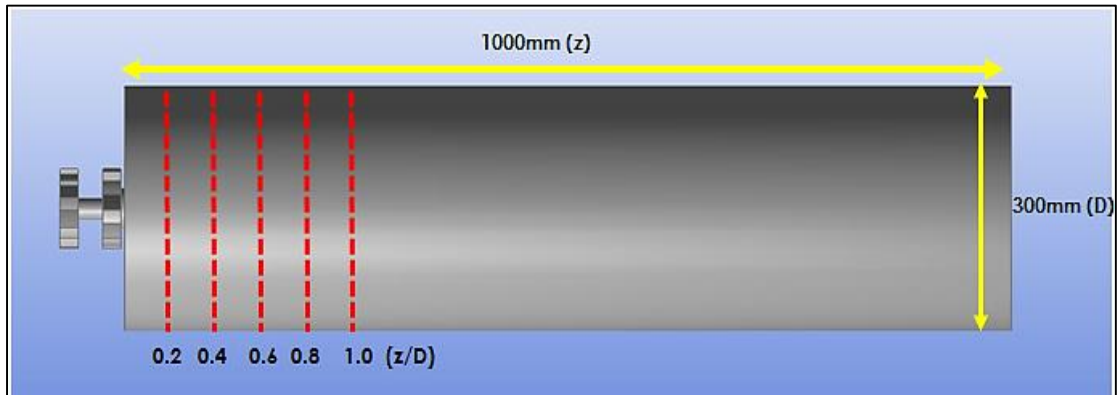


Figure 4 Dimension of CFD model with flow field measurement cross section (z/D)

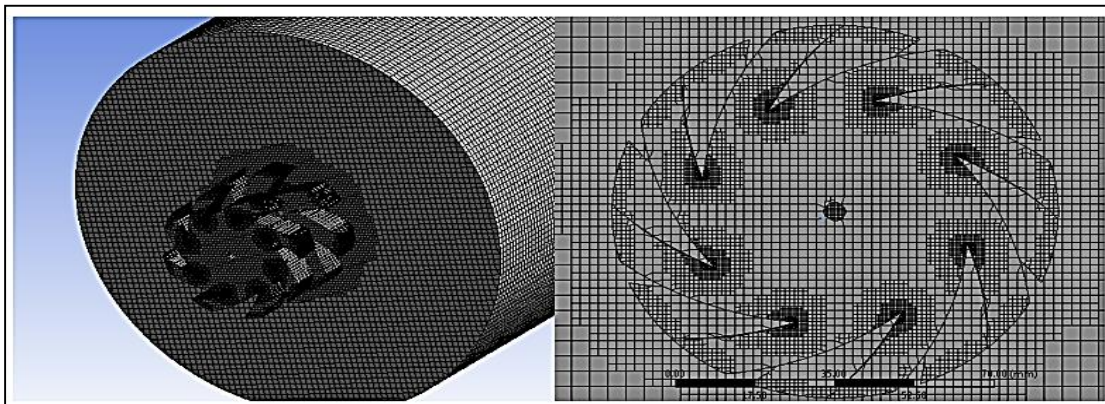


Figure 5 Meshing style for CFD combustion model

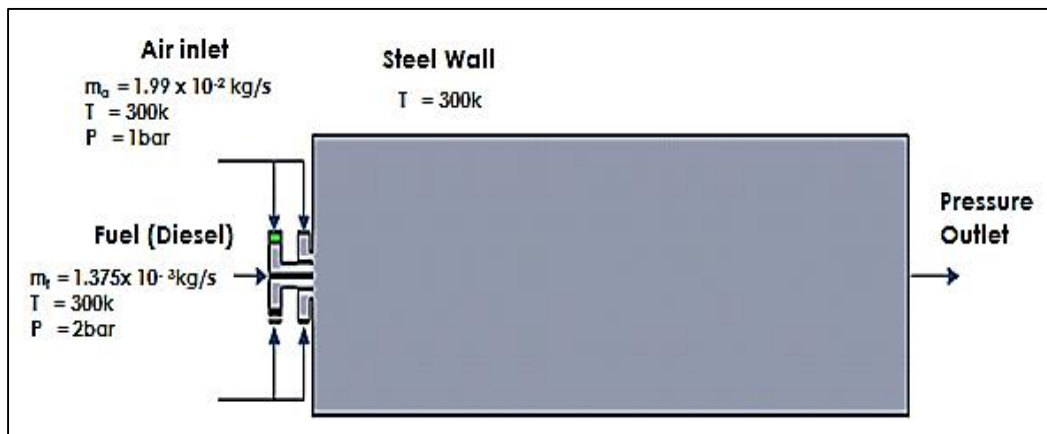


Figure 6 Boundary conditions in CFD combustion model

2.2.2 Boundary Conditions

This simulation conducted as a chemical reaction or a combustion flow. The fuel type that was used is diesel ($C_{10}H_{22}$). This fuel is the same as that used in the actual combustion tests. For this analysis, the equivalent ratio ϕ , was set to 1.0 only.

The temperatures for fuel and air were set to ambient temperature of 300 K. The pressure for air inlet was 1 bar and the pressure for the fuel was set at 2 bar. The mass flow rate for air inlet was 1.99×10^{-2} kg/s and for fuel was 1.375×10^{-3} kg/s as detailed in Figure 6. The wall of the combustor was made from stainless steel.

2.2.3 Fluent Numerical Solutions

The turbulence model for this simulation was focused only on k-epsilon model. It was run on standard, RNG and Realizable models. Based on these three types of model, the results of temperature compared with the experimental test results. This is to determine which model can accurately predicts the results.

Species for this combustion was applied as non-premix combustion. This means that the fuel and air was mixed in the combustor, thus creating a chemical reacting flow. In the solution method, the solver used was pressure-based with Semi Implicit Method for Pressure Linked Equations (SIMPLE) algorithm. The Quadratic Upstream Interpolation for Convective Kinetics (QUICK) scheme was implemented in the spatial discretization setting in order to enhance the result accuracy.

3.0 RESULTS AND DISCUSSION

3.1 Grid Independency Test

The grid independency test was conducted in order to ensure that all CFD simulation results were not affected by the grid quality and cell size. The test was performed using three different grid cell sizes that are 0.6×10^6 , 0.9×10^6 and 1.3×10^6 number of cells. The cell structure used for the meshing of the geometry generated was the hexahedral shape.

The Reynolds Number (Re) used for this study was 0.6×10^6 . Based on the test results as shown in Figure 7, it can be concluded that these two different cell sizes gave similar values and that it is acceptable to use G2 as optimum grid size for the rest of the combustion simulation study. In order to get good result in swirling flow, the grid proposed is 1×10^6 [19]. The convergence criteria was reached when the residuals was reduced four orders of magnitude [19].

3.2 Validation of Simulation

Combustion simulation result was compared with the actual experimental result in order to ensure the CFD solver producing valid prediction that is able to be a reference for further study using this type of combustor. The temperature profile during combustion was

compared with the three type of turbulence models that are Standard k- ϵ , RNG k- ϵ and Realizable k- ϵ .

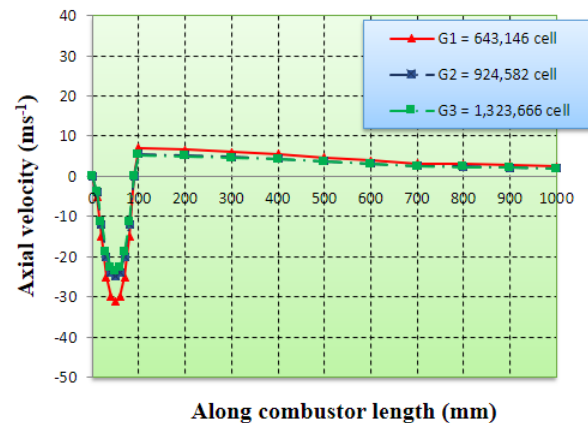


Figure 7 Axial velocity at three different Grid size

Based on the result presented in Figure 8, it can be observed that the Realizable k- ϵ gave the most similar trend for temperature profile in this simulation study. This turbulent model consists the improvement of transportation equation compared to the standard and RNG models. It also solved mathematically the constraint in the Reynolds' normal stress. Realizable k- ϵ model is suitable to be used in swirling, recirculation and high-pressure drop flow [20]. Thus, all further simulation study will use Realizable k- ϵ turbulence model. This temperature profile was based on steady flow.

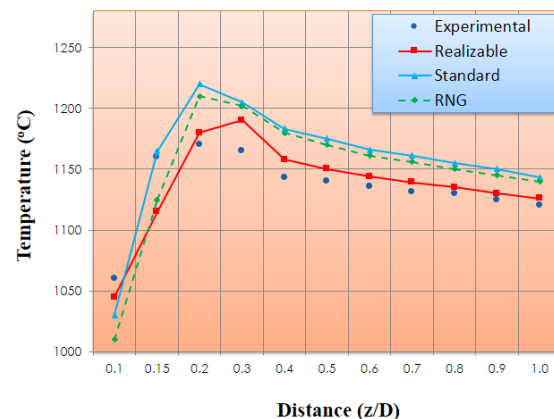


Figure 8 Flame temperature profile comparison at steady flow with $\phi = 1.0$

3.3 Flame Profile

Figure 9 shows the flame shape or profile comparison between experimental test and CFD simulation. The experimental test was conducted by previous researchers using combustion chamber testing rig in UTM Combustion laboratory at Faculty of Mechanical Engineering [8]. The $30^\circ/40^\circ$ swirler combination has the lowest swirl angle when compared to the $30^\circ/50^\circ$ and

30°/60° swirler combinations. The 30°/60° swirler combination exhibited the shortest flame length.

The swirl divergent angle between 50° and 60° almost comparable and just differs by less than 10°. The flame pattern that was simulated by CFD has similar profile compared to the experimental testing.

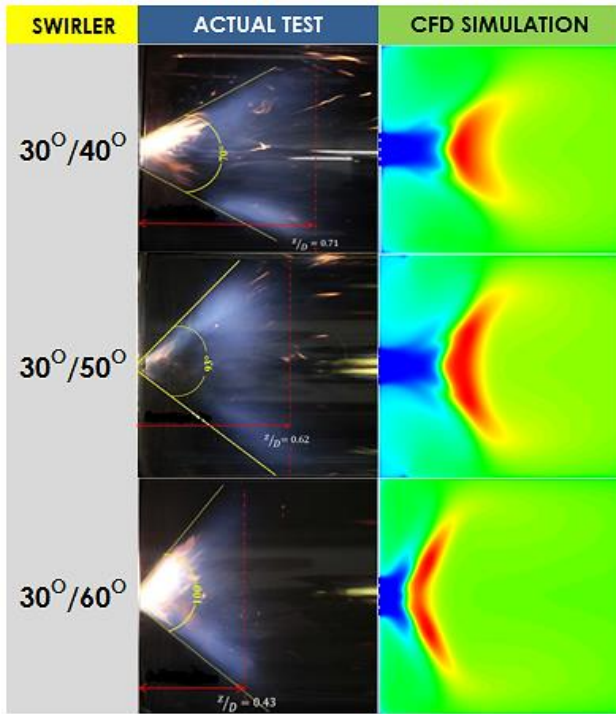


Figure 9 Flame profile and temperature contour comparison between experimental and CFD simulation

Swirler combination of 30°/40° has the lowest swirl angle due to the lowest swirl number amongst these swirler combinations. This confirmed that the swirl number plays an important role in determining the flow field pattern and performance in a combustion chamber. The temperature value from CFD was always higher than the experimental testing [21].

3.4 Velocity Profile

Figure 10 shows the different axial velocities for the three different combinations of double radial swirler at steady flow injection. The 30°/40° swirler combination generated the lowest swirl angle compared to the 30°/50° and 30°/60° combinations. This is because the 30°/40° swirler combination has smaller geometrical swirl number. The 30°/60° has strong axial and swirl velocities thus generating higher swirl number.

It has been shown that the swirling flow is located mostly at the primary combustion zone that contributes advantages in term of air/fuel mixing increment.

Based on Figures 11 and 12, the 30°/60° swirlers have the highest central reversal flow at cross section (z/D=0.2) with velocity of 87m/s, followed by 30°/50° that generates 82m/s.

At the cross section of (z/D=0.4), the 30°/40° swirler generates the highest reversal flow of 73m/s that is close to the center of the combustor. Compared to the 30°/50° and 30°/60° swirlers at this section, the peak value of reversal flow was quite close to the combustor wall that indicate the reversal flow was wide and spread until the wall of combustor.

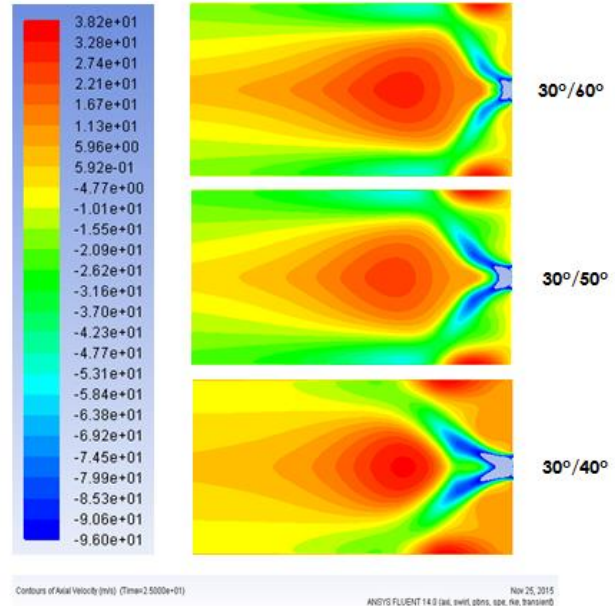


Figure 10 Axial velocity profiles at steady flow injection

By referring to Figures 12 and 13, it can be seen that the flow pattern at (z/D= 0.6 to 1.0) for swirlers 30°/50° and 30°/60° are almost similar. For the 30°/40° swirler, it can be considered that the swirling flow was weak to generate flow reversal since there was no convergence achieved compared to the other swirler combinations.

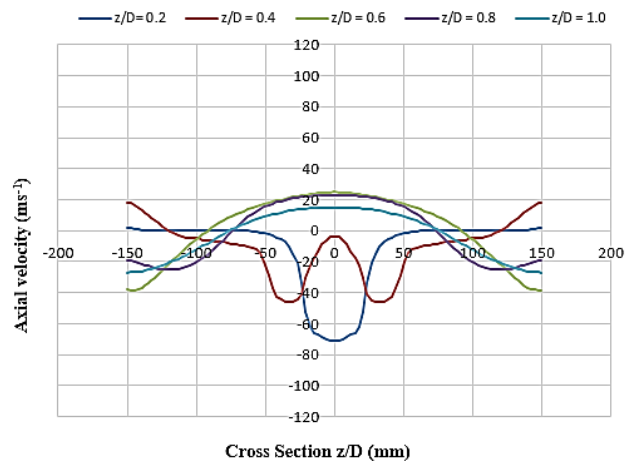


Figure 11 Axial velocity at several cross sections in combustor for Swirler 30°/60°

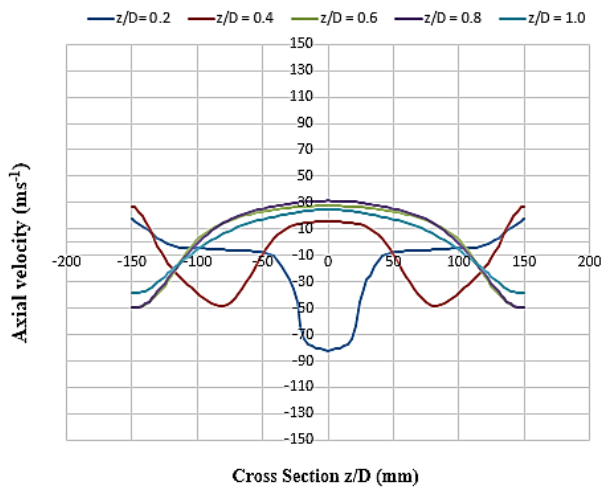


Figure 12 Axial velocity at several cross sections in combustor for Swirler 30°/50°

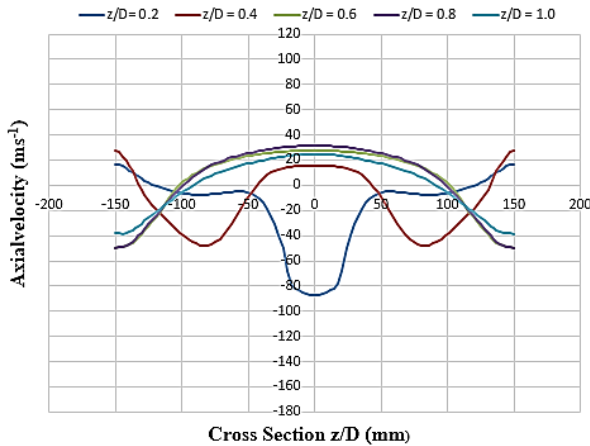


Figure 13 Axial velocity at several cross sections in combustor for Swirler 30°/40°

Figure 14 shows the condition of axial central reversal flow for 30°/60° swirler. It is apparent that the flow reversal was located at the center and near the wall of the combustor. The flow reversal almost covered the entire combustion primary zone.

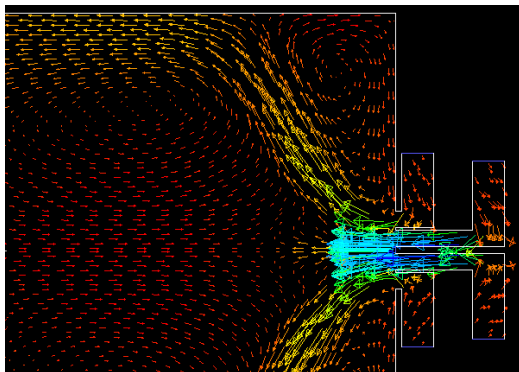


Figure 14 Flow velocity vector along the combustor for 30°/60° swirler

3.5 NOx and CO Profile Comparison

The CFD results for the production of NOx emission (Figure 15) during combustion show the average error percentage of about 22%. This disparity may be caused by the chemical reaction equations that were used, the actual air/fuel mass flow rate and the error given by the gas analyser. The CFD result was based on the chemical reaction generated and derived based on the Probability Density Function (PDF) in the solver and boundary conditions that were set.

The result for CO emissions (Figure 16) in this comparison was better than that for NOx results. The average error percentage was about 17.8% only. According to the predictions, changes in the swirl number highly affected the temperature and thus affected the NOx production [22]. This may contribute to the error obtained for NOx emission generated.

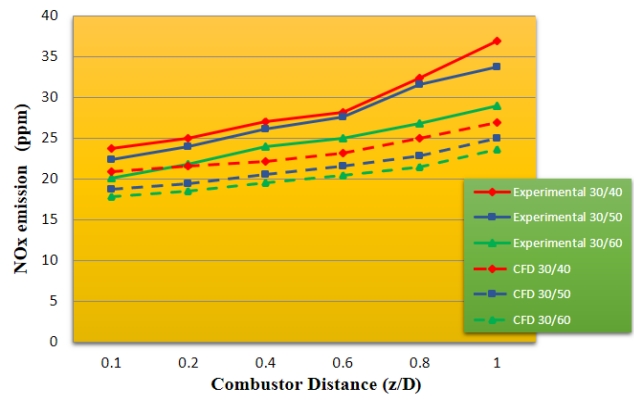


Figure 15 NOx concentration versus the distance along the combustion chamber

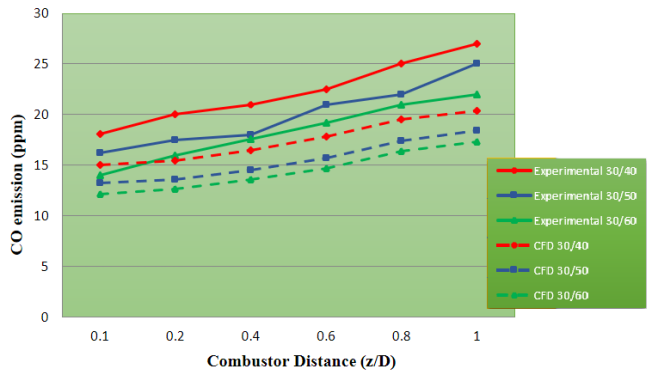


Figure 16 CO concentration versus the distance along the combustion chamber

3.6 Turbulence Intensity

One of the important criteria to observe for the flow field pattern and performance in the simulation is to analyse the turbulence intensity for all swirler combination.

Based on Figures 17 until 19, the turbulence intensity for the 30°/40° swirler combination was quite different compared to the 30°/50° and 30°/60° double swirler

combinations. The swirl divergent angle was smaller than 90° and with a longer turbulence stream.

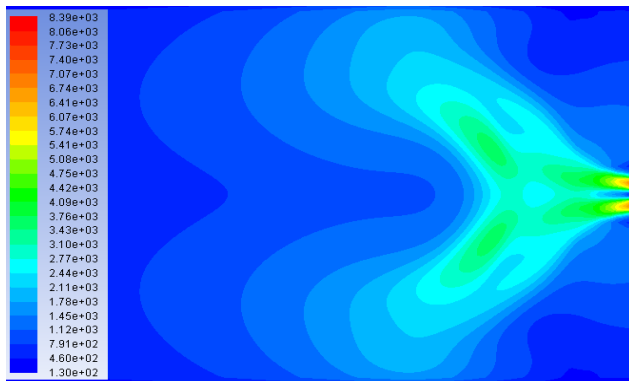


Figure 17 Turbulence Intensity along the combustor for $30^\circ/40^\circ$ swirler

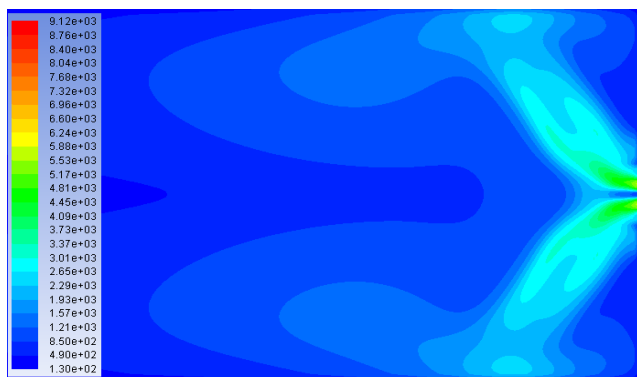


Figure 18 Turbulence Intensity along the combustor for $30^\circ/50^\circ$ swirler

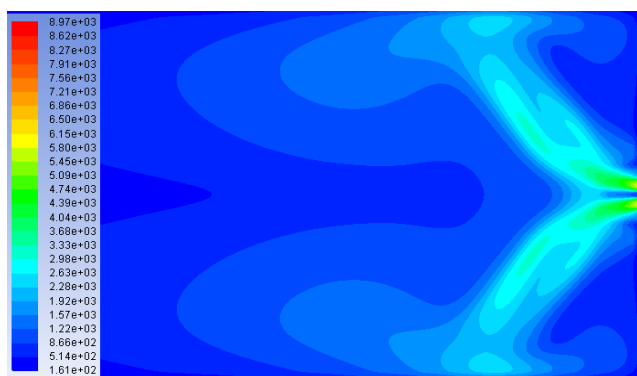


Figure 19 Turbulence Intensity along the combustor for $30^\circ/60^\circ$ swirler

The $30^\circ/60^\circ$ double swirler combination generates the highest turbulence flow for this simulation and confirming the fact, that enhancement of the swirl number contributes a positive effect in the stream contour of flow pattern.

4.0 CONCLUSION

This study presents a comparison of flow field pattern for three double radial swirler combinations, between experimental tests and CFD simulations. The similar pattern results between experimental and simulation have been achieved.

Regarding the velocity of induced air and fuel during combustion process, it can be described that the axial velocity for all double swirler combinations generate high swirling flow and turbulence. The double swirler will enhance the reaction between air and fuel and was predicted to have a short residual time to combust and reducing the emissions in exhaust gases. The $30^\circ/60^\circ$ swirler creates higher central reversal zone flow in combustor.

All swirler combinations produce high turbulence intensity with the same and steady mass flow rate.

Acknowledgement

The authors would like to thank the Ministry of Higher Education of Malaysia for sponsoring this Masters by research study and the Research Management Centre (RMC), Universiti Teknologi Malaysia (project vote number: 17H47) for awarding research grant to undertake this project.

References

- [1] Yoon, J., Kim, M. K., Hwang, J., Lee, J. and Yoon, Y. 2013. Effect of Fuel-Air Mixture Velocity on Combustion Instability of a Model Gas Turbine Combustor. *Applied Thermal Engineering*. 54: 92-101.
- [2] Mohamad Shaiful, A. I. and Nazri, M. 2014. Effect of Velocity Variation at High Swirl on Axial Flow Development inside a Can Combustor. *Jurnal Teknologi*. 71(2): 19-24.
- [3] Durox, D., Moeck, J. P., Bourgooin, J. F., Morenton, P., Viallon, M., Schuller, T. and Candel, S. 2013. Flame Dynamics of a Variable Swirl Number System and Instability Control. *Combustion and Flame*. 160(9): 1729-1742.
- [4] Benim, A. C., Iqbal, S., Meier, W., Joos, F. and Wiedermann, A. 2017. Numerical Investigation of Turbulent Swirling Flames with Validation in a Gas Turbine Model Combustor. *Applied Thermal Engineering*. 110: 202-212.
- [5] Jaafar, M., M. Nazri, K. Jusoff, M. S. Osman, and M. S. A. Ishak. 2011. Combustor Aerodynamic using Radial Swirler. *International Journal of Physical Sciences*. 6(13): 3091-3098.
- [6] Rahim, R., dan M. N. M. Ja'afar. 2015. Kesan Sudut Pusaran Terhadap Pembakaran Menggunakan Pemusar Jejarian Dwi Aliran. *Jurnal Teknologi*. 77: 8 37-45.
- [7] Tanaka, S., Shimura, M., Fukushima, N., Tanahashi, M. and Miyauchi, T. 2011. DNS of Turbulent Swirling Premixed Flame in a Micro Gas Turbine Combustor. *Proceedings of the Combustion Institute*. 33(2): 3293-3300.
- [8] Saqr, K. M., Aly, H. S., Sies, M. M. and Wahid, M. A. 2011. Computational and Experimental Investigations of Turbulent Asymmetric Vortex Flames. *International Communications in Heat and Mass Transfer*. 38(3): 353-362.
- [9] Saqr, K. M., Kassem, H. I., Aly, H. S. and Wahid, M. A. 2012. Computational Study of Decaying Annular Vortex Flow using the $R\epsilon/k-\epsilon$ Turbulence Model. *Applied Mathematical Modelling*. 36(10): 4652-4664.
- [10] Bulat, G., Jones, W. P. and Marquis, A. J. 2014. NO and CO Formation in an Industrial Gas-Turbine Combustion Chamber

- using LES with the Eulerian Sub-Grid PDF Method. *Combustion and Flame*. 161(7): 1804-1825.
- [11] Zeng, Z., Ren, J., Liu, X. and Xu, Z., 2015. The Unsteady Turbulence Flow of Cold and Combustion Case in Different Trapped Vortex Combustor. *Applied Thermal Engineering*. 90: 722-732.
- [12] Zhu, X., Li, R., Li, D., Zhang, P. and Qian, R. 2015. Experimental Study and RANS Calculation on Velocity and Temperature of a Kerosene-Fueled Swirl Laboratory Combustor with and without Centerbody Air Injection. *International Journal of Heat and Mass Transfer*. 89: 964-976.
- [13] Ishak, M. S. A., M. N. M. Jaafar, and Omar W. Z. 2014. The Effect of Inlet Air Preheat on CO and NO Production in the Combustion of Diesel in Canister Burner. *Jurnal Teknologi*. 71(2): 163-172.
- [14] Duwig, C. and Iudiciani, P. 2014. Large Eddy Simulation of Turbulent Combustion in a Stagnation Point Reverse Flow Combustor using Detailed Chemistry. *Fuel*. 123: 256-273.
- [15] Gicquel, L. Y., Staffelbach, G. and Poinso, T. 2012. Large Eddy Simulations of Gaseous Flames in Gas Turbine Combustion Chambers. *Progress in Energy and Combustion Science*. 38: 782-817.
- [16] Eldrainy, Y. A., Saqr, K. M., Aly, H. S. and Jaafar, M. N. M. 2009. CFD Insight of the Flow Dynamics in a Novel Swirler for Gas Turbine Combustors. *International Communications in Heat and Mass Transfer*. 36(9): 936-941.
- [17] Zhang, T. H., Liu, F. G. and You, X. Y. 2014. Optimization of Gas Mixing System of Premixed Burner Based on CFD Analysis. *Energy Conversion and Management*. 85: 131-139.
- [18] Syred, N. and Beer, J. M. 1974. Combustion in Swirling Flows: a Review. *Combustion and Flame*. 23: 143-201.
- [19] Kianpour, E., Sidik, N. A. C. and Bozorg, M. A. S. M. 2013. Thermodynamic Analysis of Flow Field at the End of Combustor Simulator. *International Journal of Heat and Mass Transfer*. 61: 389-396.
- [20] Zhou, H., Yang, Y., Liu, H. and Hang, Q. 2014. Numerical Simulation of the Combustion Characteristics of a Low NOx Swirl Burner: Influence of the Primary Air Pipe. *Fuel*. 130: 168-176.
- [21] Hu, B., Huang, Y., Wang, F. and Xie, F. 2013. CFD Predictions of LBO Limits for Aero-Engine Combustors using Fuel Iterative Approximation. *Chinese Journal of Aeronautics*. 26(1): 74-84.
- [22] İlbaş, M., Karyeyen, S. and Yilmaz, İ. 2016. Effect of Swirl Number on Combustion Characteristics of Hydrogen-Containing Fuels in a Combustor. *International Journal of Hydrogen Energy*. 41(17): 7185-7191.